

Relationship Between Cepheid and Tully-Fisher Distance Calculations

John C. Hodge¹

Pisgah Astronomical Research Institute, 1 PARI Drive, Rosman, NC, 28772

scjh@citcom.net

Michael W. Castelaz

Pisgah Astronomical Research Institute, 1 PARI Drive, Rosman, NC, 28772

mcastelaz@pari.edu

ABSTRACT

A correlation between (1) the difference between the Tully-Fisher calculated distance and Cepheid calculated distance for a target galaxy and (2) the magnitude and distance of galaxies close to the target galaxy is described. The result is based on a sample of 31 galaxies that have published Cepheid distances with a wide range of characteristics and distances from 2.02 Mpc to 49.7 Mpc. The energy impinging on a target galaxy from neighboring galaxies is related to the residual between Tully-Fisher and Cepheid distance calculations of the target galaxy. These relations have four different zones dependent on the value of the impinging energy. The correlation coefficients are 0.77, 0.87, 0.81, and 0.98, respectively. This relationship is of interest not only for its ability to reduce the Tully-Fisher to Cepheid distance residual but also because it suggests neighboring galaxies have a strong influence on the apparent luminosity of galaxies and it suggests the Tully-Fisher relationship assumption that the intrinsic mass to intrinsic luminosity ratio is constant among galaxies is valid for $z < 0.006$.

Subject headings: cosmology:theory— galaxies:distances and redshifts— galaxies:fundamental parameters

¹Visiting from XZD Corp., 3 Fairway St., Brevard, NC, 28712

1. INTRODUCTION

The residual between the Cepheid distance calculation D_c for a galaxy and the Tully-Fisher relationship (TF) distance calculation D_{tf} for the galaxy varies among galaxies (Shanks 1997; Shanks et al. 2002). The residual can be small for some galaxies or greater than the sum of the errors of each calculation for other galaxies. The D_{tf} to a target galaxy is determined by relating the 21-cm line width at 20 percent of the peak value W_{20} corrected for the inclination between our line of sight and the target galaxy's polar axis i with the absolute magnitude M in various wavelength bands (Tully et al. 1998). The D_c is based on the observation that pulsating Cepheid stars in a galaxy have a M related to their pulse period. Cepheids obey very well defined relations and so make excellent standard candles (Binney & Merrifield 1998)(page 415). This paper uses D_c as standard distances. In this Paper, the influence of neighboring galaxies on M is investigated for the first time. A remarkably tight correlation is found relating the illumination of neighboring galaxies to $(D_c - D_{tf})$ for redshift $z < 0.006$. Since this result was obtained with the assumption that the mass of a galaxy is constant over time, there may be a fundamental physical mechanism regulating the mass of galaxies. Also, the TF assumption that the intrinsic mass to intrinsic luminosity ratio is constant among galaxies (Aaronson, Huchra, & Mould 1979) is valid for $z < 0.006$.

The object of this paper is to examine the effect of neighboring galaxies on D_{tf} . Thereby, the residual between D_c and D_{tf} distances may be reduced. The approach is to (A) develop an equation from the Principle of the Conservation of Energy describing the influence of neighboring galaxies on D_{tf} , (B) choose galaxies with published Cepheid distances, and (C) apply the model to the target galaxies.

2. MODEL

The light emitted from a galaxy is energy from the galaxy. The Principle of the Conservation of Energy in a galaxy requires,

$$\Delta M c^2 + E_{out} = E_{in} + \epsilon, \quad (1)$$

where ΔM is the rate of change of mass M in the target galaxy, c is the speed of light, E_{out} is the rate energy radiates from the target galaxy, E_{in} is the rate of transmittal of energy from another galaxy into the target galaxy, and ϵ is the rate of intrinsic energy production from mass conversion processes in the target galaxy.

McLure & Dunlop (2002) found that the mass in the central region of a galaxy is 0.0012 of the mass of the bulge. Ferrarese and Merritt (2002) reported that about 0.1% of a galaxy's

luminous mass is at the center of galaxies and that the density of supermassive black holes (SMB) in the universe agrees with the density inferred from observation of quasars. Merritt & Ferrarese (2001); Ferrarese and Merritt (2002) found similar results in their study of the relationship between the mass M_\bullet of a SMB and dispersion velocity σ of a galaxy. Ferrarese (2002) found a tight relation between rotation velocity v_c and bulge velocity dispersion σ_c which is strongly supporting a relationship of the center force with total gravitational mass of a galaxy. Either the dynamics of many galaxies are producing the same increase of mass in the center at the same rate or a mechanism exists to evaporate (convert to radiated energy) the mass increase that changes as the rate of inflow changes. The rotation curves imply the dynamics of galaxies differ such that the former is unlikely. Merritt & Ferrarese (2001b) suggested a feedback mechanism must exist in such a way that $\Delta \log(M_\bullet) \approx 4.5 \Delta \log(\sigma)$. Therefore, M is assumed to remain constant, the matter in an incremental cylinder shell of a galaxy is constant, and $\Delta M = 0$. Whatever the source of matter in a galaxy, the energy content of the inflowing matter equals ϵ . Constant mass in a galaxy and the observation of ϵ implies there is inflowing matter.

Another source of energy for a galaxy is from other galaxies as E_{in} . The energy transfer from other galaxies can be (A) in the form of photons E_a , (B) in the form of potential energy E_p from gravitational forces of other galaxies. The E_a component is dependant on the surface area cross section of the target galaxy presented to the other galaxy, the distance between galaxies, and the M of the other galaxies. The E_p is a conservative field. If the matter in an incremental cylinder shell of the target galaxy is constant, then $E_p = 0$. The heat change caused by the movement of a galaxy as a whole in a potential field is assumed to be negligible in the B band.

Therefore, conservation of energy implies the only radiated energy observed is from re-radiated energy from neighboring galaxies and from ϵ ,

$$E_{out} \propto 10^{\frac{-M}{2.5}} = K_a E_a + K_e \epsilon, \quad (2)$$

where K_a and K_e are proportionality constants of E_a and ϵ , respectively [herein called “Conversion Efficiencies” (CE)] and $E_{in} = K_a E_a$. The CE’s represent the fraction of energy transmitted in the measurement band of M relative to the available energy. Hence, $K_a E_a$ is the observed luminosity originally from neighbor galaxies re-emitted from a target galaxy and $K_e \epsilon$ is the observed intrinsic luminosity of the target galaxy. Since ϵ will vary among galaxies, $K_e \epsilon$ will also vary among galaxies. The K_a is a function of the target galaxy’s absorption per unit surface area and the re-emitted light per unit absorption. Since the HI mass to total mass ratio increases systematically from giant galaxies towards dwarf galaxies (Karachentsev, Makarov, & Hutchmeier 1999), K_a may change accordingly. Therefore, it is reasonable to assume that the K_a also changes with ϵ .

Consider the $(D_c - D_{tf})$ as an error in D_{tf} . The error rate is defined as the correction factor C_f ,

$$C_f \equiv \frac{D_c - D_{tf}}{D_{tf}}, \quad (3)$$

or,

$$D_c = D_{tf}(1 + C_f). \quad (4)$$

Consider the attenuation of energy is a constant factor F_a of the light from the target galaxy. The term on the left side of equation (2) is the luminosity calculated by the TF relation. If D_c is the true distance, the last term on the right side of equation (2) is the intrinsic luminosity that would be calculated using D_c . Therefore, $D_{tf} = F_a 10^{-M/2.5}$ and $D_c = F_a K_e \epsilon$. Substituting these relations into equation (3) and solving equations (2) and (3) for C_f yields,

$$C_f = \frac{K_a E_a}{K_e \epsilon - K_a E_a}. \quad (5)$$

A binomial expansion of the denominator of equation (5) yields,

$$C_f = K_s E_a + K_i, \quad (6)$$

where K_i is the sum of second and higher order terms and is approximately a constant and,

$$K_s = \frac{K_a}{K_e \epsilon}. \quad (7)$$

If $K_a \propto K_e \epsilon$ among galaxies, then a plot of C_f versus E_a will yield a linear relationship. That is, for each E_a there corresponds one and only one value of C_f . Therefore, C_f is a functional relationship of E_a . The function may have discontinuities and gaps but it is still one relationship.

Galaxies with a measured D_c can be used as calibration galaxies to calculate K_s and K_i . Then equations (4) and (6) can be used to calculate a distance corresponding to a D_c .

3. DATA AND ANALYSIS

The criteria for choosing galaxies for the analysis are (1) the galaxy has a published Cepheid distance, (2) the distance to the galaxy must be large enough that the Milky Way's contribution to E_a is negligible, (3) the distance to the galaxy must be large enough that the contribution of the peculiar velocity to the redshift z measurement is relatively small, and (4) either a published total apparent magnitude in the in the B band m_b or a published

total apparent corrected I-band magnitude m_i must be available for both the target and close galaxies.

The data and references for the 31 target galaxies is presented in Table 1. The morphology type data was obtained from the NED database². The de Vaucouleurs radius R_{25} , the m_b (“btc” in the Leda database), the m_i (“itc” in the Leda database), and W_{20} data came from the LEDA database³. The value of “btc” for close galaxies was used since I band data is generally unavailable. In 35 of the 310 close galaxies, the “btc” was not available in LEDA. The B band magnitude from NED, which is not corrected, was then used. In 14 galaxies m_b was unavailable from either database. These galaxies were deleted from the calculation and the next closest galaxy added to have 10 galaxies for the calculation. The m_b for the galaxies which used the NED magnitude have relatively high values. Therefore, their significance was low. The D_c was taken from Freedman et al. (2001) distance modulus except as noted in Table 1.

The sample of target galaxies included (A) low surface brightness (LSB), medium surface brightness (MSB), and high surface brightness (HSB) galaxies, (B) galaxies with a range of W_{20} values from 61 kms^{-1} to 607 kms^{-1} , (C) LINER, Sy, HII and less active galaxies, (D) galaxies which have excellent and poor agreement between D_{tf} and D_c , (E) a distance range from 2.02 Mpc to 49.7 Mpc, (F) field and cluster galaxies, and (G) galaxies with rising, flat, and declining rotation curves.

For each of the target galaxies, the D_{tf} was calculated using the equations from Tully et al. (1998). The W_{20} value was corrected for inclination, and used for W_R^i in the TF equations. For target galaxies, D_{tf} was calculated using total apparent corrected I band magnitude (“itc”) and equations except for the galaxies IC 4182, NGC 1326A, NGC 4496A, and NGC 4571. For these target galaxies, the “btc” and equations were used since “itc” data was unavailable in LEDA.

NGC 3031 and NGC 3319 are HSB galaxies with significant differences between D_{tf} and D_c measurements. NGC 1365 has a rapidly declining rotation curve with a decline of at least 63% of the peak value (Jörsäter & van Moorsel 1995). NGC 2841 is a candidate to falsify the MODified Newtonian Dynamics (MOND) model (Bottema et al. 2002). A distance greater than 19 Mpc, compared to the measured D_c of 14.1 Mpc, or a high mass/luminosity ratio is needed for MOND. The D_{tf} value of 25.5 Mpc given herein is compatible with MOND. NGC 3031 has significant non-circular motion in its HI gas (Rots & Shane 1975). NGC 3198

²The NED database is available at: <http://nedwww.ipac.caltech.edu>.

³The LEDA database is available at: <http://leda.univ-lyon1.fr>.

is well suited for testing theories since the data for it has the largest radius and number of surface brightness scale lengths (van Albada et al. 1985). NGC 4321 has a very asymmetric HI rotation curve and is “lopsided” (Knapen et al. 1993) in the disk region of the galaxy.

The NED database was used to assemble a list of galaxies closest to each of the target galaxies. The selection of close galaxies used the Hubble Law with a Hubble constant H_o of $70 \text{ km s}^{-1} \text{ Mpc}^{-1}$ and galactic z to calculate the distances to galaxies. The angular coordinates were taken from the NED database. For each target galaxy, the distance from each target galaxy to each of the other galaxies was calculated. The neighbor galaxies with the smallest distance were chosen as the close galaxies.

The uncertainty of the value of H_o is high. The use of H_o herein is restricted to only the selection of the neighbor galaxies. As the relative distances become larger, the distance uncertainty increases if only because of a greater variation in peculiar velocity. Therefore, there is a practical upper limit on the number of galaxies that can be used to evaluate E_a . If too few close galaxies are used, E_a will be underestimated. The number of close galaxies found to produce the highest correlation coefficient was 10.

For each close galaxy, the distance from the Milky Way to the galaxies $D_{g(jk)}$ (in Mpc) was calculated by,

$$D_{g(jk)} = \frac{z_{g(j)}}{z_{c(k)}} D_{c(k)}, \quad (8)$$

where $z_{g(j)}$ is the z of the j^{th} close galaxy, $z_{c(k)}$ is the z of the k^{th} target galaxy, and $D_{c(k)}$ is the D_c of the k^{th} target galaxy. A bold character denotes a vector and the same character without the bold denotes the magnitude of the vector. The sub ($\text{}$) indicated the letters enclosed are indices identifying the galaxies of the calculation. The vector direction of $\mathbf{D}_{g(jk)}$ was calculated from coordinates found in the NED database.

The distance $R_{(jk)}$ from the j^{th} close galaxy to the k^{th} target galaxy was calculated as,

$$R_{(jk)} = |\mathbf{R}_{(jk)}| = |\mathbf{D}_{c(k)} - \mathbf{D}_{g(jk)}|. \quad (9)$$

Calculating $D_{g(jk)}$ by the method of equation (8) reduces the error of $R_{(jk)}$ compared to other methods.

The total absolute magnitude $M_{(j)}$ of the j^{th} close galaxy was calculated,

$$M_{(j)} = m_b - 25 - 5 \log(D_{g(jk)}). \quad (10)$$

The cross sectional area of the k^{th} target galaxy A presented to the j^{th} close galaxy was calculated by,

$$A_{(jk)} = \pi R_{25}^2 \sin I_{(jk)}, \quad (11)$$

where $I_{(jk)}$ is the angle between the k^{th} target galaxy’s plane and $\mathbf{R}_{(jk)}$ (see Figure 1) and is calculated from i from the LEDA database (“incl”), the position angle “pa” from the LEDA database and the orientation sign as noted in Table 1 in the i column. The dependence of $A_{(jk)}$ on a target galaxy’s orientation relative to a close galaxy may be significant. The sign indicates whether the galaxy’s polar axis is rotated clockwise or counterclockwise from our line of sight about the major axis when viewed from the easterly side of the major axis. Figure 2 is a diagram depicting a hypothetical example of our view and a close galaxy’s view of the same galaxy. Our view (a and c in Figure 2) is independent of whether the northwest side of the target galaxy is closer or farther than the southeast side. The close galaxy will have one of two possible views depending on the orientation of the target galaxy. In view b of Figure 2 the close galaxy is located in the plane of the target galaxy with a positive i and $A_{(jk)}$ is minimal. With a negative i sign, $A_{(jk)}$ as depicted in view d of Figure 2 has a significant value.

The E_a was calculated as,

$$E_{a(k)} = \sum_{j=1}^n 10^{\frac{-M_{(jk)}}{2.5}} \frac{A_{(jk)}}{4\pi R_{(jk)}^2}, \quad (12)$$

where n is the number of galaxies included in the calculation. In this case, $n = 10$. The unit of measure of E_a is in flux units ($erg\ cm^{-2}\ s^{-1}$).

The procedure to determine the sign of i is as follows. (A) The difference ΔE_a between the value of E_a with a positive i and E_a with negative i was calculated for each target galaxy. (B) Nine target galaxies had a ΔE_a of less than 5 in the second significant figure, 17 had a ΔE_a of less than 1 in the first significant figure. The sign of i was of minimal significance for these galaxies. (C) Since the relative position of these 17 galaxies on the C_f versus E_a plot changed little, these 17 target galaxies established the initial E_a ranges and the initial constants of equation (6). (D) The sign of i of the remaining target galaxies was determined such that their value of E_a was within their error limits of one of the initial lines. (E) The sign of i of the initial 17 galaxies was re-chosen such that the value was closest to the line. (F) The equations of the lines were recalculated.

The results are presented in Table 1.

A plot of C_f versus E_a is shown in Figures 3 and 4. The galaxies form into four distinct Conversion Efficiency Type (CET) relations, labeled CET 1, CET 2, CET 3, and CET 4. The characteristics of each CET is tabulated in Table 2. The statistical test of variance of the line and E_a of the sample galaxies (F test) for all CET regions is 0.99. The projections of the lines intersect at $(E_a, C_f) = (550 \pm 50\ erg\ cm^{-2}\ s^{-1}, -0.54 \pm .07)$.

The error $\partial E_a(D_c)$ in E_a due solely to the error in D_c is also listed in Table 1 for each

target galaxy. Table 2 shows the range of E_a and $\partial E_a(D_c)$ for each CET. The choice of sign of i could also have been done using the criteria that values of E_a and $\partial E_a(D_c)$ be within the ranges specified in Table 2.

The large error in NGC 4603 is a result of the unusually large published error in D_c . NGC 4535 was the only galaxy where the line was outside its error limits. NGC 4535 could fit nearly as well in CET 4 with a positive i sign and an out of range $\partial E_a(D_c)$. If the sign of i of NGC 4535 is positive, NGC 4535 is closer to CET 4, the correlation coefficient of CET 3 increases to 0.94, and the $\partial E_a(D_c)$ is in the CET 3 range. Therefore, if CET 4 is selected for NGC 4535, the $\partial E_a(D_c)$ and the E_a are in different ranges. Hence, NGC 4535 was considered to be in CET 3.

The analysis presented herein depends on the Cepheid distances being secure, standard distances. Freedman et al. (2001) adopted a metallicity PL correction factor of $-0.2 \pm 0.2 \text{ mag dex}^{-1}$. Ferrarese et al. (2000) assumed the PL relation was independent of metallicity. If the Cepheid distances used are from the earlier work of Ferrarese et al. (2000), which are higher than Freedman et al. (2001), the correlation coefficients are -0.74, 0.89, 0.85, and 0.98 for the CET 1, CET 2, CET 3, and CET 4 zones, respectively, and the slopes and intercepts of the new equations are within 3σ of the slopes and intercepts of the equations of Table 2. Thus, the theory and the result presented herein appear robust relative to systematic variation in the Cepheid distances.

The analysis also depends on the Hubble law. There is considerable uncertainty in the value of H_o . The attempt to minimize this uncertainty was to consider only galaxies near the target galaxy and to calculate the distances between galaxies using the ratio of z values. This assumes that the H_o varies little around each target galaxy. The effect of the error in H_o is limited to a selection bias. Using $H_o = 80 \text{ km s}^{-1} \text{ Mpc}^{-1}$ produced no significant change in the results.

NGC 3621, NGC 3319, and NGC 4535 are outliers in CET 1, CET 2, and CET 3, respectively. These three galaxies have a more negative C_f than their respective theoretical lines. The removal of these galaxies from consideration yields the modified correlation coefficient, modified K_s , and modified K_i listed in Table 3.

4. DISCUSSION

Shanks et al. (2002) suggested the Cepheid distances may be underestimated due to metallicity and magnitude incompleteness. Also, the sign and value of a possible metallicity correction factor is uncertain (Freedman et al. 2001). As the difference between Ferrarese

et al. (2000) and Freedman et al. (2001), the effect will be to change only the slope and intercept of the CET equations.

The existence of four E_a zones is unexplained. It should be noted that for each zone K_s and K_i are constants distinct from other zones. We speculate that since K_s has discrete values, equation (7) implies K_a , $K_e\epsilon$, or both must have discrete values, also. That is, the values are not continuously variable. If K_a and $K_e\epsilon$ depend on internal characteristics of a galaxy such as chemical composition, then the gap between CET zones and a discrete value K_s implies E_a must influence at least two of K_a , K_e , or ϵ . We speculate that other galaxies influence parameters internal to a galaxy including chemical composition. Another unexplained characteristic is the ratio of the slopes. The ratio of the slopes is 4.24 between CET 3 and CET 2 and 3.65 between CET 4 and CET 3 (both approximately 4). Also unexplained is the convergence of the linear equations to $(E_a, C_f) = (550 \pm 50 \text{ erg cm}^{-2} \text{ s}^{-1}, -0.54 \pm .07)$.

Since the $C_f - E_a$ relationship has excellent correlation coefficients without NGC 3621, NGC 3319, and NGC 4535, some of the assumptions made in developing the model may be invalid for these galaxies. NGC 3319 is rich in HI (Moore & Gottesman 1998) and NGC 4535 is poor in HI (Giovanelli & Haynes 1983). However, if a galaxy has different absorption due to HI, then the $K_e\epsilon$ should also change since HI is a fuel for emission, also. Another intriguing possibility is that there are three more CET zones. The additional zones would consist of (A) NGC 2090 and NGC 3031, (B) NGC 1326A and NGC 3319, and (C) NGC 1365 and NGC 4535. The functional relationship would be maintained. Another method to determine the orientation (sign) of each galaxy, more data, and reduced error are needed.

The choice of sign of the inclination angle is the most subjective part of the data. In some cases such as NGC 0300, the difference in E_a causes a change of CET zone which leaves the C_f nearly the same. As expected, a sign change has greater effect on the galaxies with one very close neighbor. If all galaxies have their inclination sign reversed, four CET categories are again formed with correlation coefficients of -0.72, 0.98, 0.91, and 0.93. However, several galaxies are outside their error limits of a line. The method is robust. The choice of sign reported herein allows this method to work. However, a better method in determining the sign would place greater confidence in the numbers.

NGC 2841 is close to the calculated line in CET 2 with a measured $C_f = 0.45$ and a calculated $C_f = 0.41$. Therefore, the model in this Paper accounts for nearly all the error in $(D_c - D_{tf})$ and D_c is much less than MOND requires. This suggests NGC 2841 is a problem for MOND.

When a galaxy's fundamental plane parameter is compared to the galaxy's luminosity,

a broader scatter and outliers (see, for example, Gebhardt et al. (2000)) result than if a parameter other than luminosity is compared. This paper suggests this is due to the effect of neighboring galaxies.

Relative to the TF equations, the model must still discover the relationship of W_{20} to the C_f . We speculate that after the adjustment for neighboring galaxies, this correction may explain the scale error found by Shanks et al. (2002) between raw Cepheid and TF distances. The TF assumption that the intrinsic mass to intrinsic luminosity ratio is constant among galaxies (Aaronson, Huchra, & Mould 1979) is valid for $z < 0.006$. The TF approach can be an even more powerful tool with C_f considered.

5. CONCLUSION

- The sample considered 31 spiral galaxies with published Cepheid distances. Predicted linear relationships between a factor expressing the relation between TF and Cepheid distance calculations and a factor expressing the amount of impinging energy from nearby galaxies were found.
- The impinging energy relation was found to have four zones depending on the amount of impinging energy. Each zone had a different linear relationship to the distance correction factor.
- The lines from the four zones projects to a common point at $(E_a, C_f) = (550 \pm 50 \text{ erg cm}^{-2} \text{ s}^{-1}, 0.54 \pm 0.07)$.
- When considering the luminosity of a galaxy, the effect of its neighbors should be considered.
- The intrinsic mass to intrinsic luminosity ratio is constant among the sample galaxies.
- The mass is constant for each of the target galaxies. Therefore, the intrinsic luminosity equals the rate of energy conversion of the mass being added to the galaxy.

This research has made use of the NASA/IPAC Extragalactic Database (NED), which is operated by the Jet Propulsion Laboratory, California Institute of Technology, under contract with the National Aeronautics and Space Administration.

This research has made use of the LEDA database (<http://leda.univ-lyon1.fr>).

We thank W. Osborne and K. Rumstay for comments and suggestions that improved the manuscript.

We acknowledge and appreciate the financial support of Cameron Hodge, Stanley, New York, and Maynard Clark, Apollo Beach, Florida, while working on this project.

REFERENCES

- Aaronson, M., Huchra, J., & Mould, J. 1979, ApJ, 229, 1
- Binney, J., & Merrifield, M. 1998, Galactic Astronomy (Princeton, NJ: Princeton University Press)(and references therein.)
- Bottema, R. et al. 2002, A&A, 393, 453
- Ferrarese, L. et al. 2000, ApJS, 128, 431 (and references therein.)
- Ferrarese, L., and Merritt, D. 2002, ApJ, 539,L9
- Ferrarese, L. 2002, ApJ, 578, 90
- Ferrarese, L., and Merritt, D. 2002, preprint (astro-ph/0206222)
- Freedman, W. L. et al. 2001, ApJ, 553, 47
- Gebhardt, K. et al. 2000, ApJ, 539, L13
- Giovanelli, R., & Haynes, M. P. 1983, AJ, 88, 881
- Jörsäter, S., & van Moorsel, G. A. 1995, AJ, 110, 2037
- Karachentsev, I. D., Makarov, D. I., & Hutchmeier, W. K. 1999, A&AS, 139, 97
- Knapen, J. H. et al. 1993, ApJ, 416, 563
- Macri, L. M. et al. 2001, ApJ, 559, 243
- Madore, B. M., & Freedman, W. L. 1991, PASP, 103, 933
- McLure, R. J., & Dunlop, J. S. 2002, MNRAS, 331, 795
- Merritt, D., & Ferrarese, L. 2001, MNRAS, 320, L30
- Merritt, D., & Ferrarese, L. 2002, *The Central Kpc of Starbursts and AGNs*, eds. J. H. Knapen, J. E. Beckman, I. Shlosman, and T. J. Mahoney (astro-ph/0107134)
- Moore, E. M., & Gottesman, S. T. 1998, MNRAS, 294, 353

Paturel, G. et al. 2002, *A&A*, 389, 19

Pierce, M. J., et al. 1992, *ApJ*, 393,523

Rots, A. H., & Shane, W. W. 1975, *A&A*, 45, 25

Shanks, T. 1997, *MNRAS*, 290, L77 (and references therein)

Shanks, T. et al. 2002, *Astro-ph/0208237* (and references therein)

Tully, R. B., et al. 1998, *AJ*, 115, 2264

van Albada, T. S. et al. 1985, *ApJ*, 295, 305

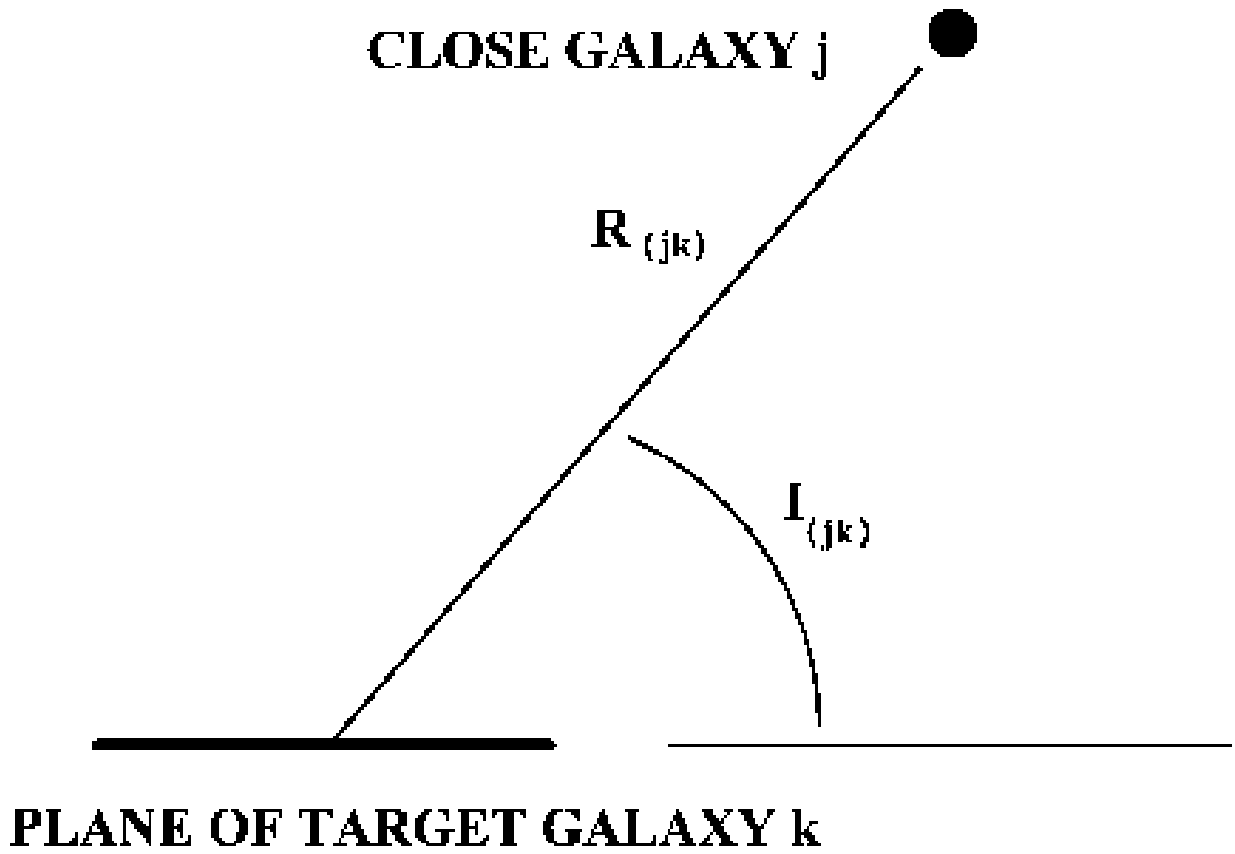


Fig. 1.— Diagram showing relationship of $R_{(jk)}$ and $I_{(jk)}$.

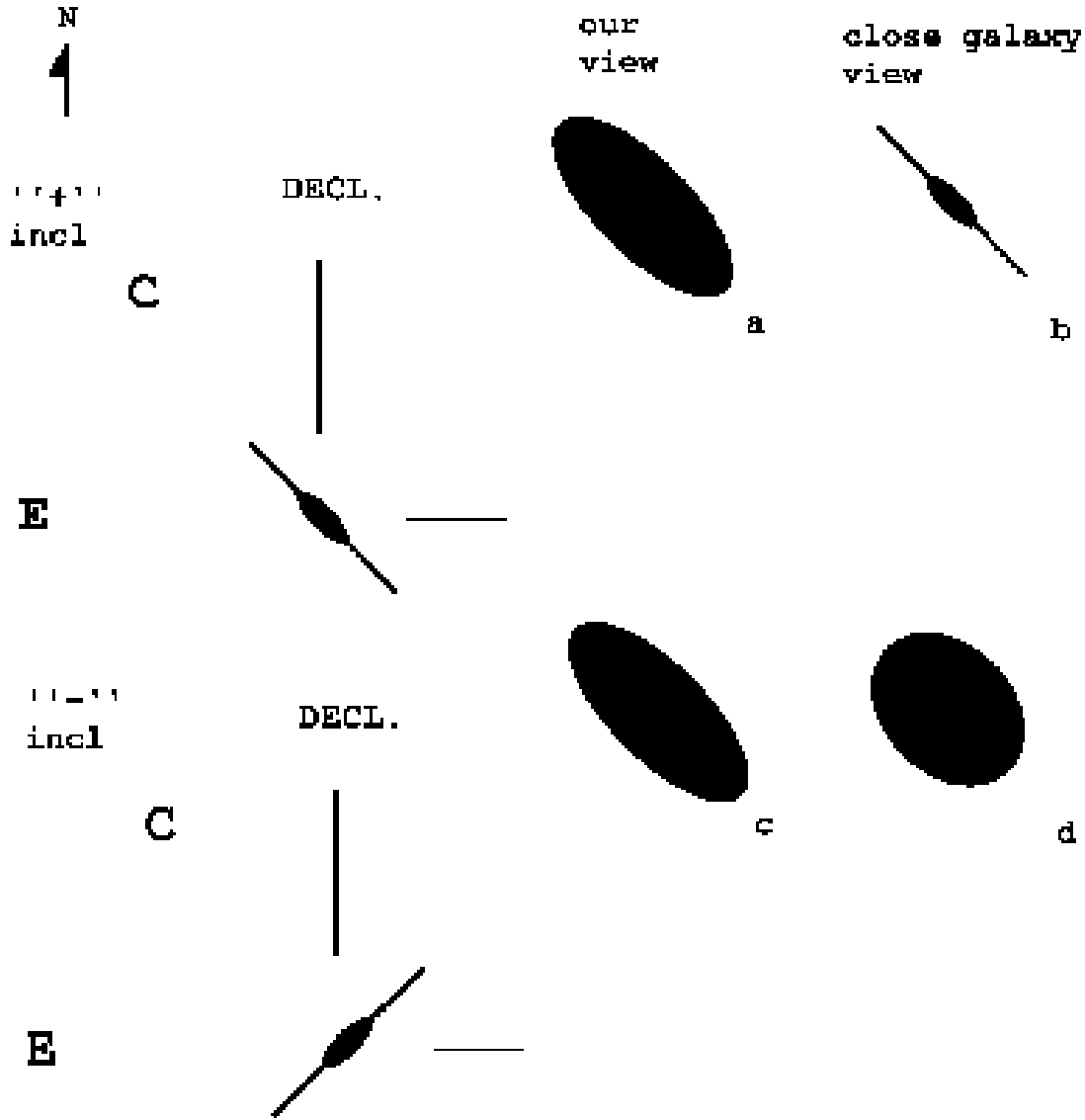


Fig. 2.— Diagram showing relationship of the sign of inclination (“incl” in the figure) on our (“E”) view of the target galaxy compared to the $A_{(jk)}$ presented to a close (“C”) galaxy. The axis labeled “DECL.” is the direction of the declination angle. The other axis is the line of sight from earth. The left diagrams show the 2 dimensional plane containing the 3 galaxies and the hypothetical relationship of the 3 galaxies.

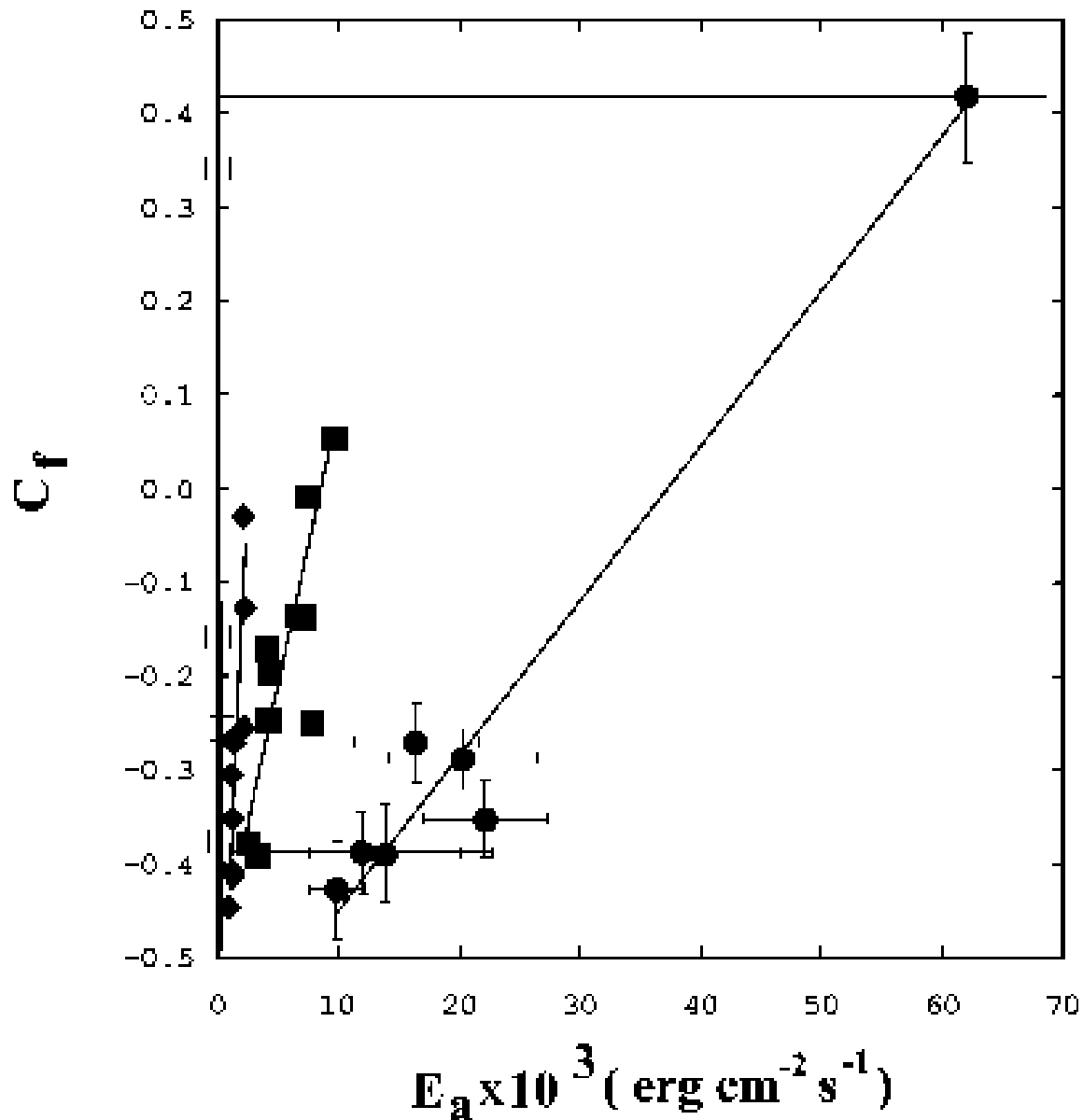


Fig. 3.— Plot of C_f versus E_a . The relationship of the four zones is shown. The lines are plots of the linear equation for each CET zone with the slopes and intercepts as listed in Table 2. The lines intersect at $(E_a, C_f) = (550 \pm 50 \text{ erg cm}^{-2} \text{ s}^{-1}, -0.54 \pm 0.07)$. Open squares designate the galaxies in CET 1, filled diamonds designate galaxies in CET 2, filled squares designate galaxies in CET 3, and filled circles designate galaxies in CET 4.

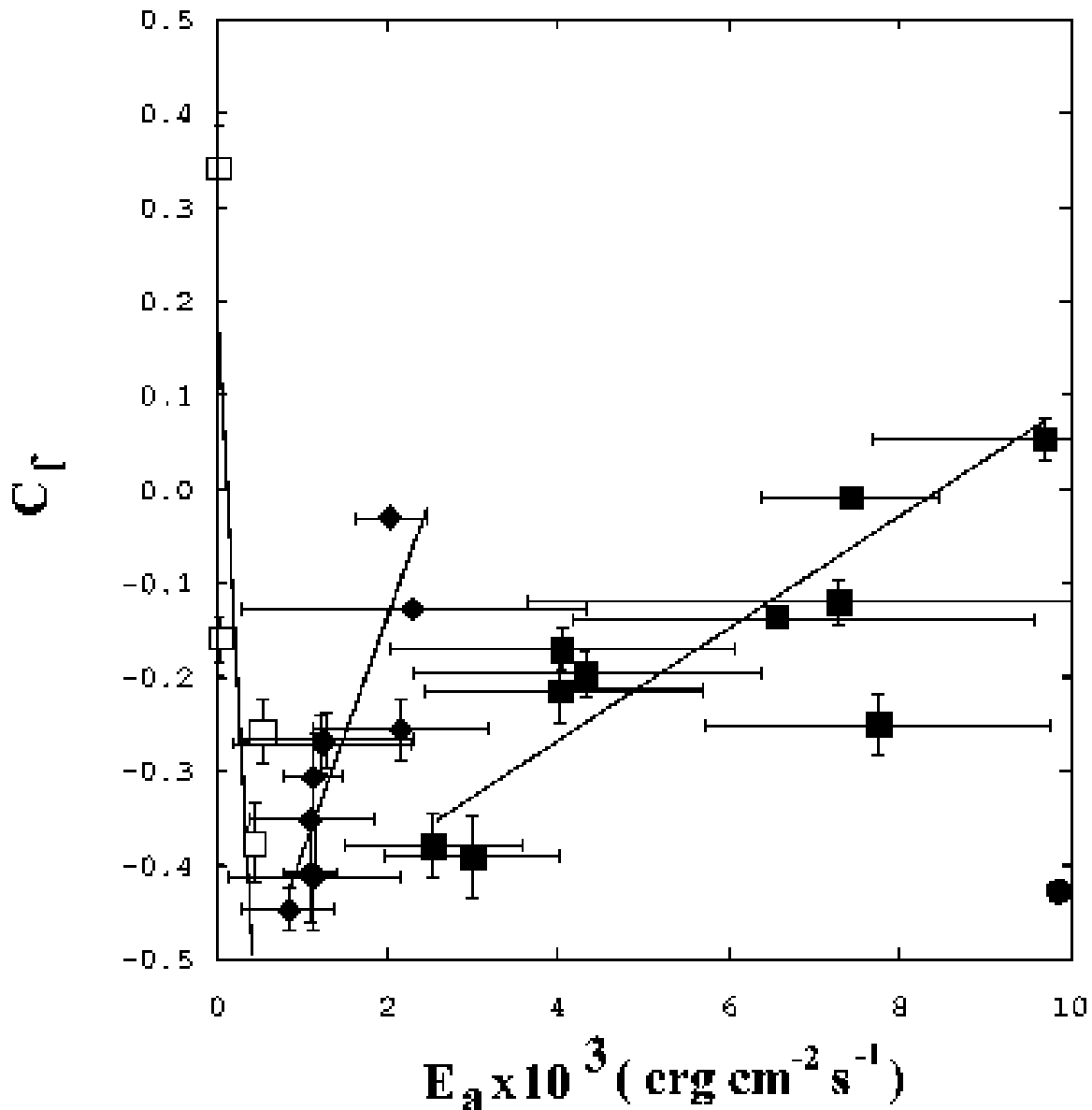


Fig. 4.— Plot of C_f versus E_a . This is an expanded view of the first 3 CET zones. The relationship of the four zones is shown in Figure 3. The lines are plots of the linear equation for each CET zone with the slopes and intercepts as listed in Table 2. Open squares designate the galaxies in CET 1, filled diamonds designate galaxies in CET 2, filled squares designate galaxies in CET 3, and filled circles designate galaxies in CET 4.

Table 1. Data for the target galaxies.

Galaxy	NED type ^a	<i>i</i> ^b	<i>m_i</i> ^c	<i>M_i</i> ^d	<i>D_{tf}</i> ^e	<i>D_c</i> ^f	<i>E_a</i> ^g	$\partial E_a(D_c)$ ^h	
CET 1									
NGC 2090	SA(rs)b HII	−68.3	9.35	−21.57	15.26±2.26	11.44± 0.21	500±	500	20
NGC 3031	SA(s)ab;LINER Sy1.8	−59.0	5.41	−23.28	5.48±0.78	3.55± 0.13	400±	100	30
NGC 3621	SA(s)d	−65.6	8.01	−21.43	7.72±1.15	6.55± 0.18	53±	40	4
NGC 5253	Im pec;HII Sbrst	+66.7	9.40	−17.50	2.40±0.36	3.25± 0.22	13±	5	1
CET 2									
IC 4182	SA(s)m	−27.1	12.27 ⁱ	−17.13 ⁱ	7.60±1.13	4.53± 0.13	1100±	300	50
NGC 0300	SA(s)d	−39.8	7.23	−20.45	3.44±0.50	2.02± 0.07	1000±	1000	60
NGC 0925	SAB(s)d;HII	−61.1	9.19	−20.68	9.41±1.39	9.13± 0.17	2000±	400	90
NGC 1326A	SB(s)m	−42.5	14.26 ⁱ	−17.04 ⁱ	18.20±2.70	16.15± 0.77	2400±	2000	200
NGC 2403	SAB(s)cd	−60.0	7.32	−21.10	4.84±0.71	3.14± 0.14	1100±	800	200
NGC 2541	SA(s)cd LINER	+66.8	10.53	−20.40	15.38±2.28	11.23± 0.26	1200±	1000	80
NGC 2841	SA (r)b;LINER Sy	+68.0	7.91	−24.12	25.51±3.78	14.07± 1.57 ^j	900±	600	200
NGC 3319	SB(rs)cd;HII	−59.1	10.39	−20.89	18.05±2.78	13.44± 0.57	2100±	1000	200
NGC 4414	SA(s)c LINER	−54.0	8.87	−23.23	26.33±3.90	16.61± 0.38	900±	1000	100
NGC 4548	SBb(rs);SY LINER	+37.0	8.89	−22.78	21.60±3.20	15.01± 0.35	1200±	300	50
CET 3									
NGC 1365	SBb(s)b Sy1.8	+57.7	8.18	−22.91	16.51±7.55	17.23± 0.40	9500±	2000	400
NGC 1425	SA(rs)b	+69.5	9.56	−22.30	23.57±3.49	20.91± 0.48	7500±	3000	300
NGC 3198	SB(rs)c	−70.0	9.22	−21.82	16.19±2.40	13.69± 0.51	4000±	2000	300
NGC 3351	SB(r)b HII Sbrst	−41.5	8.32	−22.58	15.15±2.25	9.34± 0.39	3100±	1000	400
NGC 3627	SAB(s)b;Sy2 LINER	+57.3	7.54	−22.79	11.62±1.73	9.38± 0.35	4900±	2000	400
NGC 4258	SAB(s)bc;Sy1.9 LINER	−72.0	7.04	−22.87	9.62±1.42	7.73± 0.26	4400±	2000	300
NGC 4496A	SB(rs)m	+48.1	11.78 ^j	−19.04 ⁱ	14.58±2.16	14.53± 0.20	7500±	1000	300
NGC 4535	SAB(s)c	−44.0	8.89	−22.57	19.64±2.91	14.80± 0.35	7900±	2000	300
NGC 4571	SA (r)d	−30.0	11.6 ^j	−20.31 ⁱ	24.06±3.57	15.15± 1.46 ^k	2600±	1000	400
NGC 7331	SA(s)b;LINER	−75.0	7.70	−23.43	16.82±2.49	14.53± 0.62	6700±	3000	600
CET 4									
NGC 3368	SAB(rs)ab;Sy LINER	+54.7	7.99	−22.70	13.76±2.04	9.87± 0.28	21000±	7000	2000
NGC 4321	SAB(s)bc; LINER HII	−30.0	8.39	−23.44	23.23±3.44	14.33± 0.47	14000±	7000	900
NGC 4536	SAB(rs)bc	−58.9	9.15	−22.32	19.66±2.91	14.46± 0.27	17000±	5000	700
NGC 4603	SA(rs)bc	−55.0	9.86	−22.86	35.05±5.20	49.70±24.15 ^l	62000±400000		80000
NGC 4639	SAB(rs)bc;Sy1.8	−52.0	10.27	−22.54	36.45±5.39	21.00± 0.79	10000±	2000	600
NGC 4725	SAB(r)ab;Sy2 pec	−54.4	8.04	−23.24	18.03±2.67	11.92± 0.33	24000±	5000	1000
NGC 5457	SAB(rs)cd	+22.0	6.99	−23.18	10.82±1.60	6.70± 0.35	12000±	11000	1000

^aGalaxy morphological type from the NED database.

^bGalaxy inclination between line of sight and polar axis (in degrees) from the LEDA database. The + or − sign signifies galaxy inclination orientation.

^cTotal apparent corrected I-magnitude “itc” of the *i*th galaxy from the LEDA database, unless otherwise noted.

^dThe absolute I-magnitude $M_I^{b,k,i}$ from Tully et al. (1998), unless otherwise noted.

^eThe calculated distance from (m-M) in Mpc.

^fDistance in Mpc from Cepheid data from Freedman et al. (2001), unless otherwise noted.

^gIn flux units $erg\ cm^{-2}\ s^{-1}$.

^hThe E_a error due solely to D_c error.

ⁱMagnitude data is total apparent corrected B-magnitude “btc” from the LEDA database and $M_B^{b,k,i}$ from Tully et al. (1998).

^jDistance is from Macri et al. (2001).

^kDistance is from Pierce et al. (1992).

^lDistance is from Paturel et al. (2002).

Table 2. Data for the Conversion Efficiency Types.

No. ^a	E_a ^b	$\partial E_a(D_c)$ ^c	Corr. ^d	K_s ^e	K_i ^f	
CET 1	4	0 - 800	0 - 40	-0.77	$-1.3(\pm 0.6) \times 10^{-3}$	0.2 (± 0.2)
CET 2	10	801 - 2400	40 - 300	0.87	$2.5(\pm 0.5) \times 10^{-4}$	-0.63(± 0.07)
CET 3	10	2401 - 9700	300 - 600	0.81	$6.0(\pm 1.0) \times 10^{-5}$	-0.51(± 0.08)
CET 4	7	9700 -	600 -	0.98	$1.6(\pm 0.1) \times 10^{-5}$	-0.61(± 0.04)

^aThe number of galaxies of the sample in each CET.

^bThe E_a range of the CET in flux units of $erg\ cm^{-2}\ s^{-1}$.

^cThe E_a error range due solely to D_c error of the CET in flux units of $erg\ cm^{-2}\ s^{-1}$.

^dCorrelation Coefficient.

^eThe best fit slope in units of $erg^{-1}\ cm^2\ s^1$ derived to make the F test greater than 0.99. The error is $1\ \sigma$.

^fThe best fit intercept derived to minimize the total difference between data and the line. The error is $1\ \sigma$.

Table 3. Data for the Conversion Efficiency Types without NGC 3621, NGC 3319, and NGC 4535.

	MOD Corr. ^a	MOD K_s ^b	MOD K_i ^c
CET 1	-0.98	$-1.5(\pm 0.3) \times 10^{-3}$	$0.38(\pm 0.10)$
CET 2	0.92	$2.7(\pm 0.4) \times 10^{-4}$	$-0.66(\pm 0.06)$
CET 3	0.93	$6.2(\pm 0.9) \times 10^{-5}$	$-0.52(\pm 0.05)$
CET 4	0.98	$1.6(\pm 0.1) \times 10^{-5}$	$-0.61(\pm 0.04)$

^aCorrelation Coefficient.

^bThe best fit slope in units of $erg^{-1} cm^2 s^1$ derived to make the F test greater than 0.99. The error is 1σ .

^cThe best fit intercept derived to minimize the total difference between data and the line. The error is 1σ .